

MODELLING FATIGUE DAMAGE GROWTH OF T700/M21 COMPOSITES UNDER HIGH FREQUENCY TESTING

M. Lasen, J.Schönthaler and D. Di Maio

Abstract

Experimental laws used to characterise fatigue in composites materials, such as Paris-Erdogan Laws or S-N curves, require time consuming testing campaigns because of their low excitation frequencies [1]. To reduce this long-lasting testing time and to improve the tracking of damage by a more sensitive characteristic physical parameter, a High Frequency Fatigue Testing (HFFT) approach [2] is proposed as an alternative. HFFT can be used at excitation frequencies which can easily be two orders of magnitude higher than low frequency testing. Low frequency fatigue testing has been the benchmark in academia and industry and its extensive use has evolved to the level of a standardised method [3]. These standards allow to obtain experimental laws and hence easily derive, for example, Energy Release Rate (ERR) and crack progression during fatigue testing. However, to build a Paris-Erdogan Law with HFFT a hybrid approach is required to estimate the ERR as the crack progresses.

A Finite Element (FE) simulation routine, written in Python and Abaqus, is designed to reproduce the experimental conditions of the HFFT as accurately as possible. This work presents the first steps to the hybrid simulation-experiment fatigue laws, by introducing the framework of the Python-Abaqus routine.

Keywords: High Frequency Fatigue Testing, Abaqus, Python, Crack growth.

1. Introduction

HFFT is a testing approach to study fatigue at high frequencies by tracking the frequency response phase of the samples measured at constant excitation frequency [2,5,6]. Its main characteristics are that the samples are run at constant excitation frequency (near the resonance), constant amplitude severity and have time-dependent varying properties. Commercially available FE fatigue software are limited in this sense, not allowing to continuously modify these properties.

To overcome these limitations, a Python routine has been designed to iteratively adapt the input conditions to the simulations, such that at every single step of crack progression the excitation resonant frequency and time-dependent damping are modified, while maintaining the FE model samples at a constant severity level.

2. The FE model.

The Abaqus FE model, in Fig. 1 has a dimension of 270x25x2.5 mm. The model is clamped in the 3 middle columns of nodes at the nodal line of the first bending vibration mode. Fig. 1 shows the Concentrated Force Loading Nodes, attached with a Kinematic Constraint. At these Loading Nodes, the forces are applied to reach the desired displacement severity level, which is measured at the indicated Measuring Reference Point, 35 mm from the Clamped Nodes at the mid-width of the sample. Three parts are defined in the model which facilitate the definition of the interfacial properties between them. The continuous orthotropic material properties used in the FE-model are summarised in 1 [4].

The elements used in the model mesh are continuum solid shell elements (CSS8, Abaqus). The thickness of the model consists of 10 plies, with a single element per layer. Each layer has a thickness of 0.25 mm. The different plies that make up the laminate are unidirectional and are stacked with the following layup: $[90_{cut}/0_{cut}/90_{cut}/0/90/90/0/90/0/90]$, where 'cut' indicates the pre-crack separating the Top Part into Left and Right. The cut-ply is offset 10 mm from the clamped centre of the

sample, represented by the Transverse Crack Nodes in Fig. 1. From there, the horizontal crack is expected to grow, horizontally between the 3rd and 4th layers, to the left and right sides of the cut-ply. The horizontal crack progression uses a VCCT fracture model, which allows to obtain the ERR at the left and right side of the transverse crack. In the Abaqus-Python routine the fracture criterion of the VCCT formulation does not determine to which side the crack is opened, the criterion is imposed after the VCCT simulation, by determining the highest ERR between the left and right sides.

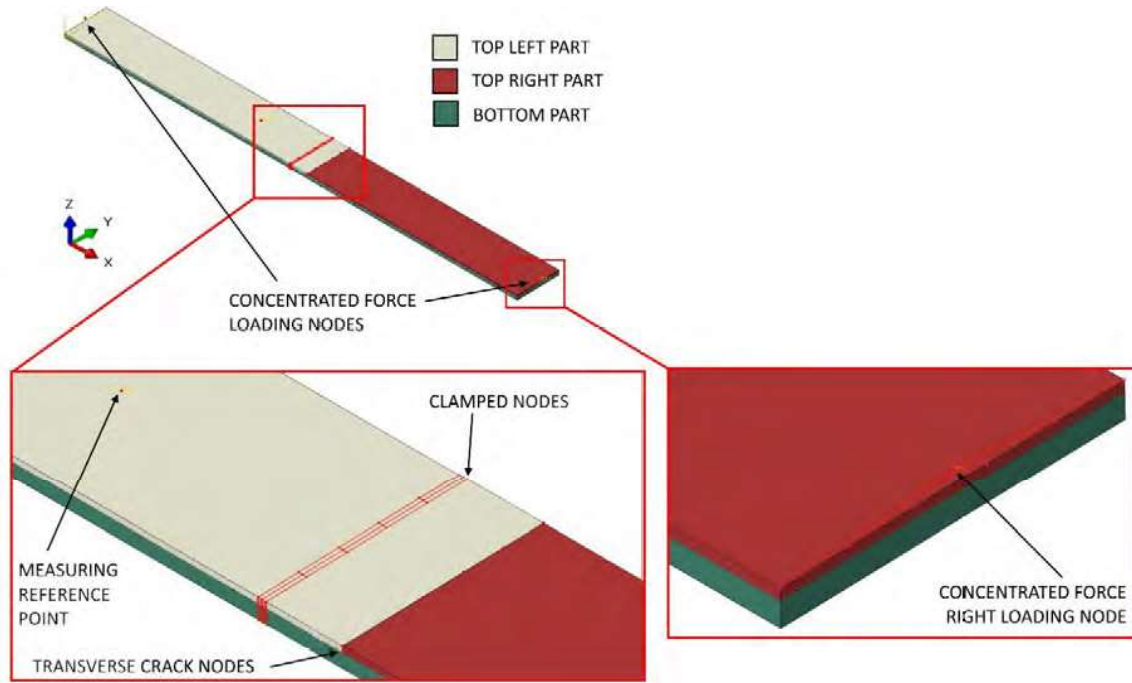


Figure 1 FE model overview and key node sets.

Table 1. T700/M21 material properties in the FE-model.

Properties	Value	Unit
Longitudinal Young's modulus E_1	124,250	MPa
Transverse Young's modulus E_2	7,660	MPa
Through-thickness Young's modulus E_3	7,660	MPa
Poisson's ratio 1-2 plane ν_{12}	0.36	-
Poisson's ratio 1-3 plane ν_{13}	0.36	-
Poisson's ratio 2-3 plane ν_{23}	0.5	-
Shear modulus 1-2 plane G_{12}	4,347.5	MPa
Shear modulus 1-3 plane G_{13}	4,347.5	MPa
Shear modulus 2-3 plane G_{23}	2,553.33	MPa
Density ρ	$1.58e^{-9}$	tonne/mm ³
Structural damping s	0.004	-

A surface-to-surface contact is defined in the transverse and horizontal cracks, with a normal hard contact and a frictional tangential behaviour with a friction coefficient $\mu = 0.35$.

3. The Python and Abaqus routine.

An overview of the Python-Abaqus is depicted in Fig. 2. The framework has 3 steps: '0: Base Case', '1: Steady State Dynamics' and '2: Static - VCCT', each of them is described in terms of the specific FE model used in each framework step, the corresponding Abaqus steps of each simulation and their key outputs.

The following subsections describe each framework step, the reasons behind them and the crack opening criterion used for the iteration of the routine.

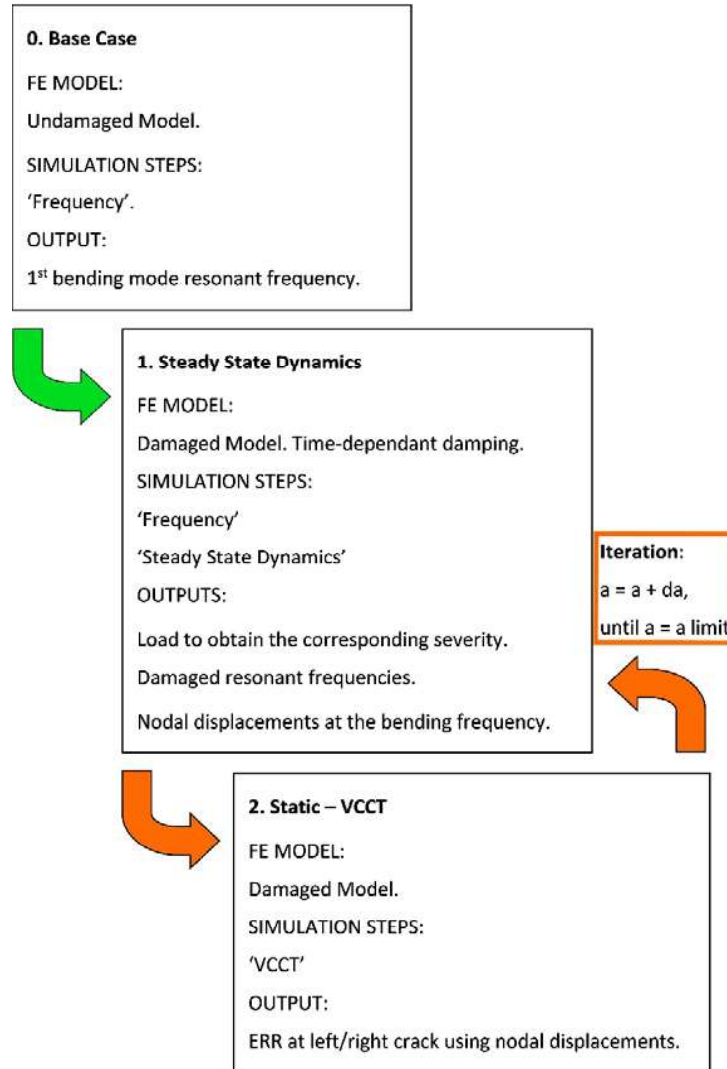


Figure 2 Python-Abaqus framework.

3.1 Framework Step 0: 'Base Case'

In Framework Step 0 (FW-step 0) an undamaged version of the FE model described in Section 1 is used, without cracks. This FW-step allows to obtain a base case of the 1st bending resonant frequency, which is used in the next FW-step.

3.2 Framework Step 1: 'Steady State Dynamics'

FW-step 1 makes use of the FE model described in Section 1. The first time the routine invokes FW-step 1, the crack opening consists of simply one element, 0.1 mm, to each side of the transverse crack. As the crack grows, the crack edge is opened uniformly across the width of the model such that the crack front is always a straight line.

To determine the right input load to match the desired severity level, the damaged FE model is run three times. The first two are run at arbitrary loading forces and the displacement severity is measured at the measuring point displayed in Fig. 1. From these two auxiliary simulations an interpolation is run to find the best representation of the loading conditions for the Steady State Dynamics, in the third simulation.

The damage accumulation needs to be reflected not only in the crack growth but also in the decay of the material properties, i.e. damping. Damping is hard to monitor during a real fatigue experiment, however, it can be studied before and after the fatigue test is done. The damping level used at each crack opening is simply an interpolation between the damping measured before and after a representative fatigue experiment.

The simulations have two Abaqus steps. (i) A 'Frequency' step is used within an arbitrary range with an upper frequency limit set by the undamaged resonant frequency from FW-step 0, from there the frequency only drops. (ii) A Steady State Dynamics (SSD) step is used to obtain the dynamic response of the damaged cases analysing two critical frequencies, the first is the current resonant frequency, obtained in (i) and the second is the previous damaged resonant frequency, at the previous crack opening.

The most important outputs of FW-Step 1 are twofold, (a) the nodal displacement at the damaged resonant frequency and (b) the dynamic response phase, phase lag between the input Concentrated Loading Force and the response of the system at the Measuring Reference Point. Studying the response allows to compare how the phase decays when damage accumulates as the crack and damping grow.

3.3 Framework Step 2: 'Static - VCCT'

FW-step 2 uses the same damaged FE model from FW-step 1. The purpose of this step is to quantify the ERR in a representative simplified loading cycle. The simplification is necessary because running iteratively a VCCT simulation to account for the ERR evolution with number of cycles, at each adjusted excitation frequency, is computationally too expensive.

To capture the behaviour of a simplified loading cycle, two Abaqus simulation are run within this step. (i) A positive bending static simulation, where the specimen is bent in a U-shape (upwards in the z-axis), and (ii) a negative bending static simulation, where the specimen is bent in an inverted U-shape. The load paths for both simulations (i, ii), are linear ('Ramp' Amplitude in Abaqus). This means that the load starts from a resting position until the prescribed nodal displacements, found in FW-step 1, are reached.

The boundary conditions holding the prescribed nodal displacements, extracted from the SSD simulations in FW-step 1 are applied sufficiently afar from the crack, otherwise it can affect the results of the total ERR. A safe window of 10.2 mm in the X-axis is used. This is considered a safe window volume since the total maximum crack length, imposed in the iteration of the Python-Abaqus routine is 5.1 mm and both left and right cracks develop sufficiently far from any of the edge's planes of this window volume. Several convergence simulations were tried against the crack opening tendency (which crack opens more left or right) to determine a safe window that does not affect this tendency.

The outputs of this step are the following, for each simulation positive and negative: the ERR of the individual modes (crack opening Mode -I, -II and III) and total ERR at each crack front, left and right. These outputs are key to determine in which direction the crack is opened in the next iteration.

3.4 Crack opening criterion in the Python-Abaqus framework.

After the last Abaqus simulation is finished, the total ERR from both positive and negative bending simulations are added at each crack front, in Python. Then the added total ERR (positive and negative) is compared between the left and right cracks, and the crack with the higher ERR is opened in the next iteration. The next iteration opens the crack front by $da = 0.1$ mm, either at the left or right crack, and the Python routine comes back to FW-step 1, with a modified FE model (larger crack, new damping level). The routine is iterated until an arbitrary total limit of 5 mm is reached, adding both left and right cracks.

4. Results

4.1 Crack progression

Fig. 3 shows the progression of the crack length to the left (blue) and right (red) of the transverse crack. The progression starts at the base of the vertical axis with the initial crack of 0.1mm at each side of the transverse crack, it then grows to the left towards the clamped nodes until it reaches a length of 2.4 mm without any growth to the right, only at this point the crack starts growing to the right.

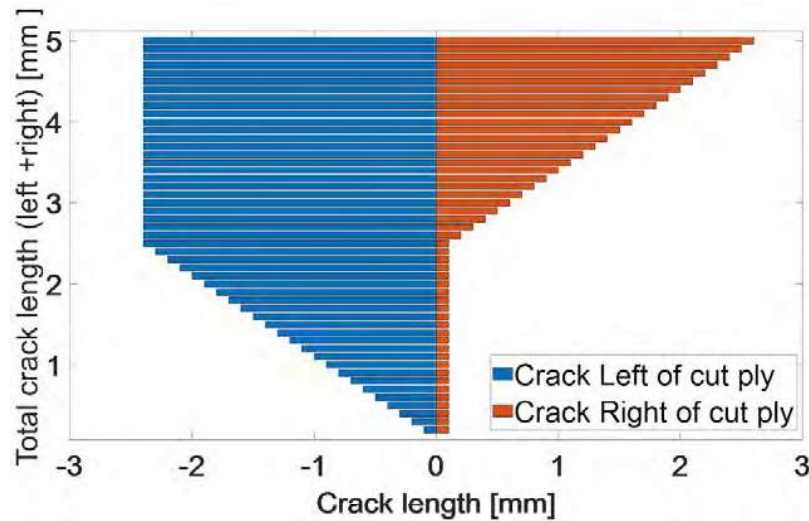


Figure 3 Simulation crack opening up to 5mm.

4.2 Phase decay

The concept of phase decay reflects on the fact that the structural strength of a component deteriorates with fatigue, this deterioration is captured in the dynamic phase response. It has previously been shown that the phase response which is the lag between the input-output (Measuring Point-Loading Point) grows as the material fatigues [5,6].

The Steady State Dynamics analysis, in FW-step 1, is performed at two key frequencies for each crack length, one is the frequency at the current damaged state, ' f_i ', and the second is the frequency of the previous damaged state, ' f_{i-1} ', see Fig. 4. This allows to determine the Instantaneous Phase decay, ϕ_I , which is the phase decay between the response vibration phase of, ϕ , at one damage case, c_i , at its resonance, f_i , and the resonance of the previous damaged case, f_{i-1} . Fig. 4 describes this concept by using simulated FRFs from the same damaged models (crack opening and evolving damping) used in the Python-Abaqus routine, it is worth noting that the Python-Abaqus routine only performs the SSD at f_i and f_{i-1} and that the FRFs shown here, with a frequency range between 116 - 122 Hz, are only used as a tool to explain the concept of phase decay. It can be seen in the close up view on the initial few damage cases

In reality, a good measurement system would compute the phase decay continuously, hence the Instantaneous Phase Decay need to be accumulated and gathered in a single curve to represent a total phase decay, as the crack grows. Fig. 5 displays the instantaneous phase decay at each crack length for a strategy considering a constant damping level equal to the initial damping state and a second strategy where the damping is continuously increased, as explained in Section 3.1.

The initial crack opening is 0.2 mm and the next opened case is 0.3 mm, therefore the first instantaneous phase decay is evaluated at $c_l = 0.3$ mm, as it is a differential with respect to the previous case. The total phase decay, $\Delta\Phi(c_l)$, is simply the sum of the instantaneous phase decay jumps from the initial case up to the current level of damage, that is, $\Delta\Phi(c_l) = -1 * [\phi_{l_i}(c_l) + \phi_{l_{i-1}}(c_l - 0.1mm) + \phi_{l_{i-2}}(c_l - 0.2mm) + \dots + \phi_l(c = 0.3mm)]$. In other words, the total phase decay is the cumulative sum of previous phase jumps. Since $\Delta\Phi$ is an arbitrary function it has been adjusted to start from 0, such that $\Delta\Phi(c = c_l)$ is the total Phase decay jump for any c_l , its sign is negative to denote the loss of strength. Fig. 5(b) shows the total Phase decay with the definition explained above.

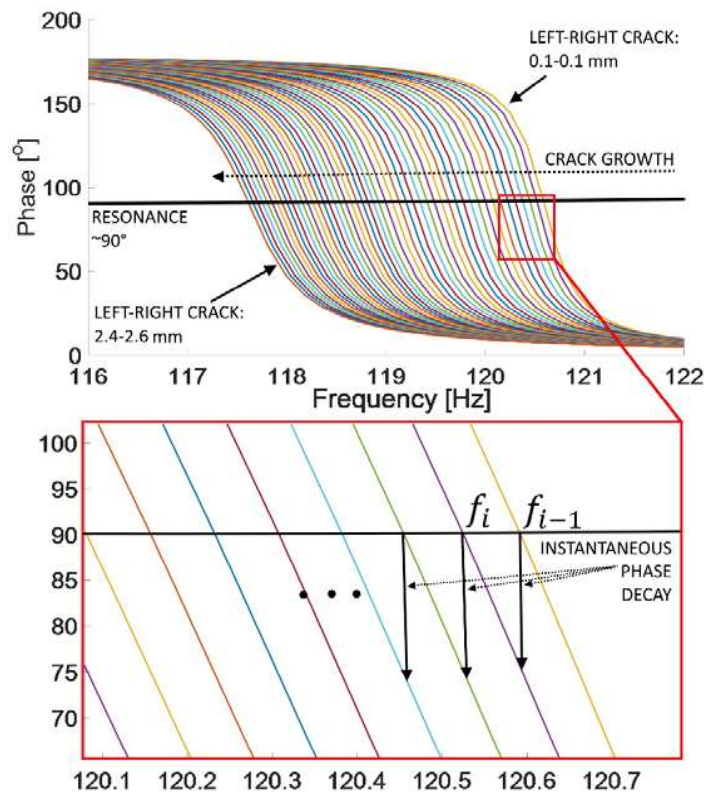


Figure 4 Concept of Phase decay explained with auxiliary FE model FRFs

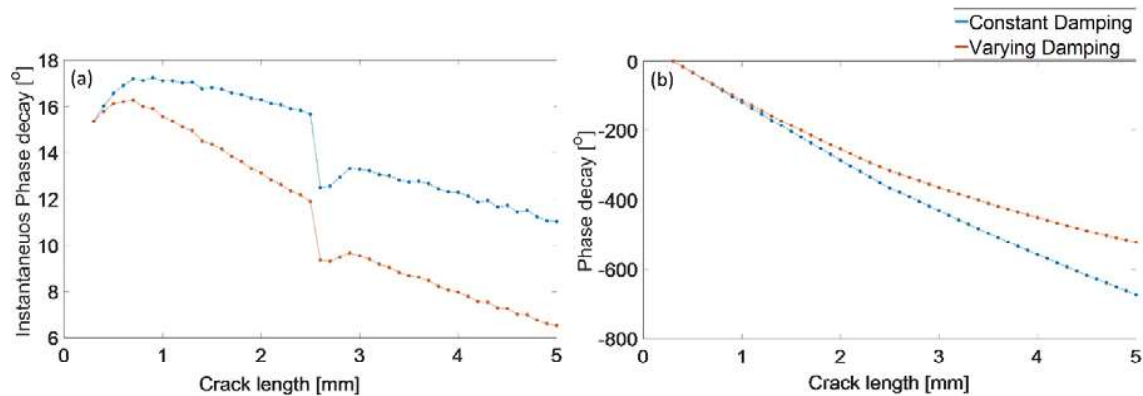


Figure 5 FE model Phase Decay. (a) Instantaneous. (b) Cumulative Total.

5. Discussion

It can be seen from Fig. 5(a) that at 2.5 mm crack length there is a sudden instantaneous phase jump. This is due to the start of the development of the right-side crack, as it can be seen from Fig 3. After that, the instantaneous phase decay of the right-side crack is the same as for the left side crack, a small increment, probably due to small or no sliding frictional behaviour at that interface, followed by a steady decrease.

In Fig. 5(b) the total accumulated Phase decay shows the effect of progressively decreasing magnitude of instantaneous phase jumps, by displaying a slight curvature.

The results in Fig. 5(a), also show the effect of a linear increasing varying damping, where the instantaneous jumps are smaller than the constant damping curve. The larger jumps in phase in the constant damping curve are reflected in the accumulated total phase decay, in Fig. 5(b), by displaying a steeper curve. The reason for this is that larger damping provides a softer response, which can be seen in Fig. 4, where the initial crack phase response is steeper around resonance than the last case of a total crack length of 5 mm.

6. Conclusions

This work shows the overview of a Python-Abaqus framework capable of representing the crack opening condition of a real HFFT experiment. Its main modelling capabilities are: (i) frequency variation due to damage, (ii) varying damping from material fatigue and (iii) constant severity level displacement throughout the entire routine.

These features provides insight into: (a) understanding of the crack growth at small scales, starting from 0.1 mm to arbitrary limits values, as well as (b) providing estimations of the ERR magnitudes for mixed modes and for two cracks, left and right, type of defects, and finally (c) a prediction of the total Phase Decay, which is an experimental signature characterising the material loss of strength from the HFFT experiments.

7. References

- [1] Silvain A. Michel, Rolf Kieselbach, Hans Jörg Martens, Fatigue strength of carbon fibre composites up to the gigacycle regime (gigacycle-composites), International Journal of Fatigue, Volume 28, Issue 3, 2006, Pages 261-270, ISSN 0142-1123, <https://doi.org/10.1016/j.ijfatigue.2005.05.005>.
- [2] Di Maio D, Magi F. Development of testing methods for endurance trials of composites components. Journal of Composite Materials. 2015; 49(24):2977-2991. doi:10.1177/0021998314558497

- [3] Fatigue standards and fracture standards - standards products - standards & publications - products & services (no date) ASTM International - Standards Worldwide. Available at: <https://www.astm.org/products-services/standards-and-publications/standards/fatigue-standards-and-fracture-standards.html> (Accessed: 29 November 2023).
- [4] Hongkarnjanakul, N., Rivallant, S., Bouvet, C., & Miranda, A. (2014). Permanent indentation characterization for low-velocity impact modelling using three-point bending test. *Journal of Composite Materials*, 48(20), 2441–2454. <https://doi.org/10.1177/0021998313499197>.
- [5] G. Voudouris *et al.*, “Experimental fatigue behaviour of CFRP composites under vibration and thermal loading,” *Int. J. Fatigue*, vol. 140, no. May, p. 105791, 2020, doi: 10.1016/j.engfracmech.2019.106626.
- [6] M. Peluzzo, D. Di Maio, A. Cammarano, and P. Castellini, “Measurement and analysis of the nonlinear stiffness of cfrp components during vibration fatigue testing,” in *Conference Proceedings of the Society for Experimental Mechanics Series*, 2020, doi: 10.1007/978-3-030-47721-9_7